Accepted Manuscript

Targeted photodynamic therapy of breast cancer cells using lactose-phthalo-cyanine functionalized gold nanoparticles

Paula García Calavia, Isabelle Chambrier, Michael J. Cook, Alan H. Haines, Robert A. Field, David A. Russell

Please cite this article as: P. García Calavia, I. Chambrier, M.J. Cook, A.H. Haines, R.A. Field, D.A. Russell, Targeted photodynamic therapy of breast cancer cells using lactose-phthalocyanine functionalized gold nanoparticles, *Journal of Colloid and Interface Science* (2017), doi: https://doi.org/10.1016/j.jcis.2017.10.030

This is a PDF file of an unedited manuscript that has been accepted for publication. As a service to our customers we are providing this early version of the manuscript. The manuscript will undergo copyediting, typesetting, and review of the resulting proof before it is published in its final form. Please note that during the production process errors may be discovered which could affect the content, and all legal disclaimers that apply to the journal pertain.

Targeted photodynamic therapy of breast cancer cells using lactose-phthalocyanine functionalized gold nanoparticles

Paula García Calavia[a], Isabelle Chambrier[a], Michael J. Cook[a], Alan H. Haines[a], Robert A. Field[b] and David A. Russell[a*]

[a]School of Chemistry, University of East Anglia, Norwich Research Park, Norwich, NR4 7TJ, UK

[b]Department of Biological Chemistry, John Innes Centre, Norwich Research Park, Norwich, NR4 7UH, UK

Corresponding author email: d.russell@uea.ac.uk

Abstract

Gold nanoparticles (AuNPs), which have been widely used for the delivery of photosensitizers for photodynamic therapy (PDT) of cancer, can be dispersed in aqueous solutions, improving the delivery of the hydrophobic photosensitizer into the body. Furthermore, the large surface of AuNPs can be functionalized with a variety of ligands, including proteins, nucleic acids and carbohydrates, that allow selective targeting to cancer tissue. In this study, gold nanoparticles were functionalized with a mixed monolayer of a zinc phthalocyanine and a lactose derivative. For the first time, a carbohydrate was used with a dual purpose, as the stabilizing agent of the gold nanoparticles in aqueous solutions and as the targeting agent for breast cancer cells. The functionalization of the phthalocyanine-AuNPs with lactose led to the production of water-dispersible nanoparticles that are able to generate singlet oxygen and effect cell death upon irradiation. The targeting ability of lactose of the lactose-phthalocyanine functionalized AuNPs was studied *in vitro* towards the galectin-1 receptor on the surface of breast cancer cells. The targeting studies showed the exciting potential of lactose as a specific targeting agent for galactose-binding receptors overexpressed on breast cancer cells.

Introduction

Carbohydrates are present on the surface of human cells in the form of glycans; oligosaccharides either bound to proteins or lipids on the surface of the cells, or free within the tissue.[1,2] The surface of the cells also presents lectins, carbohydrate-binding proteins that recognize glycans in a specific manner *via* their carbohydrate-recognizing domain (CRD).[1–3] Glycans and lectins are involved in many important roles in an organism,[4] including embryonic development, cell growth, differentiation and adhesion, apoptosis, cell signaling, cell-cell

1

recognition, interactions between cells and the extracellular matrix and the regulation of host-pathogen interactions, amongst others.[1–3,5] It is known that changes in the phenotypic distribution of glycans and lectins is linked with cancer.[3,5–7] The changes in the expression of glycans and lectins can be related to the under- or over-expression of the enzymes responsible for their biosynthesis, glycosyltransferases and glycosidases, as well as their localization within the Golgi apparatus, to the expression of oncofetal antigens only present in embryonic cells and cancer cells, but not in healthy adult tissue, or to changes in the carbohydrate structure.[2,3,6,8] Therefore, the aberrant glycosylation patterns in cancer cells can be used for targeted cancer therapy. Such targeting could be performed using carbohydrates to target endogenous lectins, *i.e.,* direct lectin-targeting or glycotargeting, or using lectins to target glycoconjugates expressed on the surface of the cancer cells, *i.e.,* reverse lectin-targeting.[9–11] Targeted cancer therapies have been reported using both direct[12–19] and reverse[20–26] lectin-targeting.

Galectins are β-galactoside-binding lectins whose over- or under-expression has been linked with cancer.[27–30] Fifteen different mammalian galectins have been identified to date.[31–33] Among them, overexpression of galectin-1 has been linked with breast cancer.[31,32,34–38] Galectin-1 has been correlated with an increased tumor aggressiveness and poor prognosis, due to its ability to promote cell adhesion, leading to metastasis.[31,32,39] It has been shown that the suppression of galectin-1 can prevent both tumor growth and metastasis.[34,36] Therefore, galectin-1 would be an ideal candidate for targeted cancer treatment, such as photodynamic therapy (PDT).

Here, we present the use of a carbohydrate, lactose, to stabilize AuNPs in aqueous solutions and to specifically target the galectin-1 receptor overexpressed on the surface of breast cancer cells. Following previous reports by our group,[20,40,41] gold nanoparticles were synthesized and functionalized with a mixed monolayer of lactose and a zinc phthalocyanine (Pc) photosensitizer. Two Pcs were explored, differing in the length of the carbon chain that connects the Pc to the gold core, consisting of either 3 or 11 carbon atoms.[42] The lactose disaccharide is made up of glucose and galactose residues. Galectin-1 has been shown to recognize and bind to both sugar units.[27] Therefore, lactose is potentially an ideal candidate as a ligand for targeted PDT.

A known lactose-containing thiol derivative,[43] **Figure 1a**, was chosen to evaluate the potential targeting towards the galectin-1 receptor on breast cancer cells. Importantly, the lactose ligand was shown to stabilize the zinc phthalocyanine-functionalized gold nanoparticles (AuNPs) in

2

aqueous solutions. The phthalocyanines used for this study were two octa-alkyl substituted zinc (II) phthalocyanines, differing in the length of the carbon chain connecting the macrocycle to the disulfide bond, either three carbon atoms (C3Pc) or eleven carbon atoms (C11Pc).[42] Schematic representations of the synthesized gold nanoparticles functionalized with a mixed monolayer of lactose and either C3Pc (lactose-C3Pc-AuNPs) or C11Pc (lactose-C11Pc-AuNPs) are shown in **Figure 1b** and **Figure 1c**, respectively.
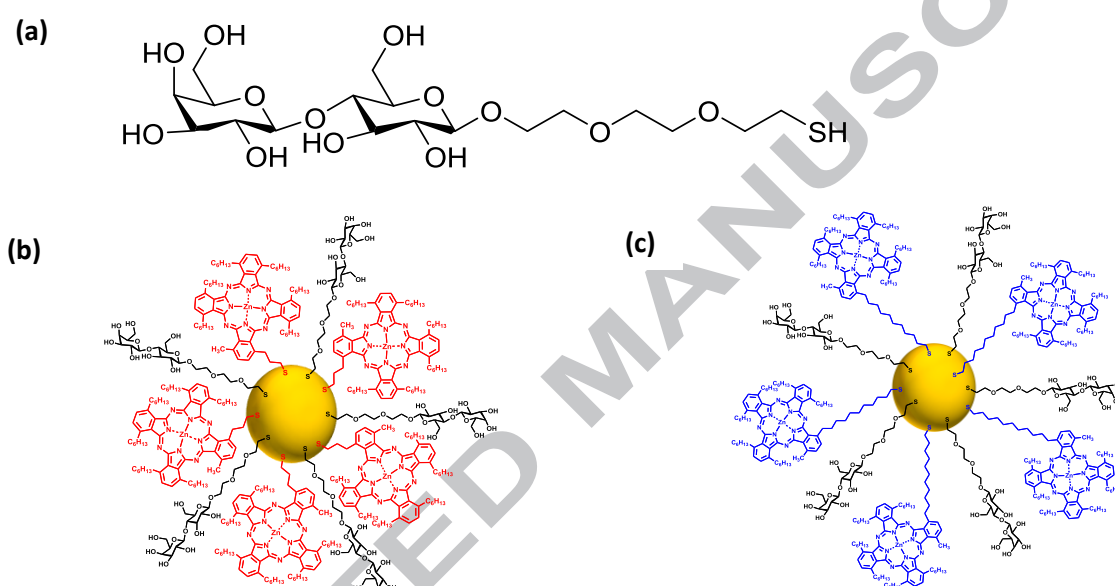

Figure 1. (a) Structure of the thiolated lactose ligand.[43] Schematic representation of the **(b)** lactose-C3Pc-AuNPs and **(c)** lactose-C11Pc-AuNPs.

Experimental

Materials and methods

All reagents were of analytical grade, used as received and purchased from Sigma-Aldrich (UK) unless otherwise stated. Tetrahydrofuran (THF) and sterilized deionized water were purchased from Fisher Scientific (UK). Sodium chloride (NaCl), phosphate buffered saline (PBS) tablets, foetal bovine serum (FBS), 75 cm^2 Nunc Easy tissue culture flasks with porous caps, Nunc 6-well multidishes, Nunc Nunclon™ Δ Surface 96-well microplates, 18 mm diameter glass coverslips and InCell ELISA colorimetric detection kit were purchased from Thermo Fisher Scientific (UK). Trypsin 0.25 % with ethylenediaminetetraacetic acid (EDTA), Gibco™ Molecular Probes™

3

soybean trypsin inhibitor, McCOY's 5A phenol red-free medium containing L-glutamine, Dulbecco's Modified Eagle Medium (DMEM), sodium pyruvate and L-glutamine (200 mM) were purchased from Invitrogen (UK). Mammary epithelial basal medium (MEBM) was purchased from Lonza (UK). CellTiter-Blue® cell viability assay was purchased from Promega (UK). Millex GP syringe drive filter units (0.22 μm) were purchased from Millipore Corporation (USA). Vivaspin™ 500 (100 kDa MWCO; PES membrane) centrifuge columns were purchased from Sartorius Stedim Biotech (UK). Thiol-dPEG®$_4$-acid (sPEG) was purchased from Stratech (UK). Staurosporine free base (> 99 %) was purchased from LC Laboratories (USA). Holey carbon film 300 mesh copper grids were obtained from Agar Scientific (UK). Rabbit monoclonal anti-galectin-1 antibody was purchased from Abcam (UK). A JDS Uniphase 633 nm Helium-Neon (HeNe) laser (10 mW) was purchased from Edmund Optics (USA). SK-BR-3 human breast adenocarcinoma cells were purchased from LGC Standards and kindly provided by Prof Dylan Edwards (Norwich Medical School, University of East Anglia, UK). MDA-MB-231 human breast adenocarcinoma and MCF-10A human mammary epithelial cells were purchased from ATCC in partnership with LGC Standards.

UV-vis spectra were recorded using a Hitachi U-3010 spectrophotometer at room temperature using quartz cuvettes with a 1 cm path length. Fluorescence excitation and emission spectra were obtained using a Hitachi F-4500 fluorescence spectrometer in quartz cuvettes with a 1 cm path length. For the plate assays, absorbance and fluorescence measurements were performed using a CLARIOstar® (BMG Labtech) microplate reader at room temperature. Transmission electron microscopy (TEM) images were obtained using a JEOL JEM-2010 Electron Microscope operating at 200 kV. Centrifugation of nanoparticle samples was performed using a Beckman Coulter Allegra™ X-22R centrifuge. Centrifugation of biological samples was performed using an Eppendorf 5810R centrifuge. Confocal microscopy was performed using a Carl Zeiss LSM 510 META confocal laser scanning microscope.

Phosphate buffered saline (PBS) was prepared by dissolving 10 PBS tablets in water (1 L). The solution was sterilized by autoclaving at 110 °C for 10 min. The final PBS solution contained Na_2HPO_4 (8 mM), potassium phosphate monobasic (KH_2PO_4; 1 mM), NaCl (160 mM), potassium chloride (KCl; 3 mM) and a pH of 7.3. MES buffer was prepared in water containing 2-(N-morpholino)ethanesulfonic acid (MES; 50 mM) and Tween-20 (0.05 %). The pH of the MES buffer was adjusted to 5.5 using aqueous solutions of NaOH (5 M) and HCl (0.6 M). Imaging medium based on Hank's balanced salt solution (HBSS) for the biological experiments was

4

prepared in water containing NaCl (120 mM), KCl (5 mM), CaCl$_2$·2H$_2$O (2 mM), magnesium chloride hexahydrate (MgCl$_2$·6H$_2$O; 1 mM), NaH$_2$PO$_4$ (1 mM), NaHCO$_3$ (1 mM), 4-(2-hydroxyethyl)piperazine-4-ethanesulfonic acid (HEPES; 25 mM), D-glucose (11 mM) and bovine serum albumin (BSA; 1 mg/mL). The pH of the imaging medium was adjusted to 7.4 using an aqueous solution of NaOH (1 M). Prior to use, all buffer solutions and imaging media were sterilized by filtration through Millex GP syringe driven filter units (0.22 µm).

Synthesis of lactose-Pc-AuNPs

Two zinc phthalocyanines (Pc) composed of either a three carbon-atom chain (C3Pc) or an eleven carbon-atom chain (C11Pc) connecting the macrocycle to the sulfur were prepared as previously reported.[44,45] Gold nanoparticles (*ca.* 3-5 nm; AuNPs) were synthesized by sodium borohydride (NaBH$_4$) reduction and functionalized with a mixed monolayer of a lactose derivative[43] together with either C11Pc or C3Pc.

C11Pc (2.43 mg; 0.95 µmol) or C3Pc (2.22 mg; 0.95 µmol) were dissolved in dry THF (1.45 mL) and left to stir at room temperature. Then, lactose derivative (1 mL; 1.31 mM in water) was added to the C11Pc solution and stirred at room temperature for 5 min. HAuCl$_4$·3H$_2$O (1.2 mg; 3.0 µmol) was dissolved in dry THF (1.2 mL), added to the C11Pc-lactose mixture and stirred at room temperature for a further 5 min. Finally, a solution of NaBH$_4$ (1.5 mg; 39.65 µmol) was prepared in water (1.2 mL) and added to the Pc-lactose solutions rapidly and under vigorous stirring. The reaction was stirred overnight (*ca.* 17 h) at room temperature in the dark at moderate speed. The resulting solution was a mixture of free Pc, AuNPs functionalized with Pc only, AuNPs functionalized with lactose only and AuNPs functionalized with both Pc and lactose. To purify the mixture, excess dry THF (6 mL) was added rapidly and under vigorous stirring, followed by centrifugation in Eppendorf tubes (1.5 mL) at 1,300 rpm for 2 min at 4 °C. The supernatant was collected and the brown pellet containing AuNPs functionalized only with lactose was discarded. The solvent mixture in the supernatant was evaporated by rotary evaporation under reduced pressure at 70 °C. For further purification, another aliquot of THF (5.4 mL) was added, followed by the same centrifugation and evaporation steps as explained previously. Once all the THF had been evaporated, MES buffer (3 mL) was added and the solubilization was assisted using an ultrasonic bath. The solution was centrifuged in Eppendorf tubes (1.5 mL) at 14,000 rpm for 30 min at 4 °C. The pellet containing free Pc and AuNPs functionalized only with Pc, and thus not soluble in an aqueous solution, was discarded. The supernatant containing the lactose-Pc-AuNPs was collected and filtered through a Millex GP

syringe driven filter unit (0.22 µm). The synthesized lactose-Pc-AuNPs were characterized using UV-vis spectroscopy, between 300-800 nm, and using TEM. A droplet of the functionalized AuNPs (20 µL) in MES buffer was placed onto a holey carbon film 300 mesh copper grid and left for 2 min to allow the nanoparticles to sediment onto the grid. Excess MES buffer was then removed by gently poking the side of the grid with filter paper. The grid was left to dry completely before imaging.

Measurement of singlet oxygen production

The lactose-Pc-AuNPs (511 µL) in MES buffer were placed in a 1.5 mL quartz cuvette together with ABMA (1 µL in methanol; 1 µM) and a magnetic stirrer bar. Oxygen was bubbled through the solution and the quartz cuvette was stoppered. The fluorescence emission spectrum of the initial solution was recorded, using an excitation wavelength of 380 nm, between 390-600 nm. The sample was then irradiated at 633 nm using a 10 mW HeNe laser for 40 min with continuous stirring. The laser was placed 50 cm away from the cuvette. The fluorescence emission spectrum of the sample was recorded every 5 min.

Synthesis of control sPEG-Pc-AuNPs

Gold nanoparticles were synthesised by $NaBH_4$ reduction and functionalized with a mixed monolayer of either C11Pc or C3Pc and thiol-dPEG®4-acid (sPEG; 282.35 g/mol), a PEG ligand with a chain simulating the length of the lactose ligand. C11Pc (2.43 mg; 0.95 µmol) or C3Pc (2.22 mg; 0.95 µmol) were dissolved in dry THF (1 mL) and left to stir at room temperature. Then, sPEG (0.51 mg; 1.8 µmol) was dissolved in water (1.9 mL), added to each phthalocyanine solution and stirred at room temperature for 5 min. $HAuCl_4 \cdot 3H_2O$ (1.2 mg; 3.0 µmol) was dissolved in water (1.2 mL), added to the Pc-sPEG mixtures and stirred at room temperature for a further 5 min. Finally, a solution of $NaBH_4$ (1.5 mg; 39.65 µmol) was prepared in water (1.2 mL) and added to the gold salt plus Pc-sPEG solutions rapidly and under vigorous stirring. The reaction was stirred overnight (*ca.* 17 h) at room temperature in the dark at moderate speed. The resulting solution was purified following the method described above for the synthesis of lactose-Pc-AuNPs.

In vitro cell work

SK-BR-3 cells were routinely cultured in McCOY's 5A phenol red-free medium containing L-glutamine and supplemented with foetal bovine serum (FBS, 10 %); MDA-MB-231 cells were

6

routinely cultured in DMEM phenol red-free medium supplemented with L-glutamine (1 %), FBS (10 %) and sodium pyruvate (1 mM); and MCF-10A cells were routinely cultured in MEBM medium supplemented with cholera toxin (100 ng/mL). All cells were grown in an incubator at 37 ˚C under a 5 % CO_2 atmosphere.

The cells were subcultured every 5 days, when they reached near confluence. The culture medium was discarded and the cells were washed with PBS (5 mL). The cells were dislodged from the flasks by addition of trypsin 0.25 % (1x) EDTA (5 mL) and incubation for either 5 min (SK-BR-3 and MDA-MB-231 cells) or 15 min (MCF-10A cells) at 37 °C under a 5 % CO_2 atmosphere. For SK-BR-3 and MDA-MB-231 cells, trypsin was deactivated by addition of the culture medium (5 mL) and removed by centrifugation at 800 relative centrifugal force (rcf) for 5 min at 21 °C. For MCF-10A cells, trypsin was deactivated by addition of soybean trypsin inhibitor (5 mL; 1 mg/mL in PBS) and removed by centrifugation at 130 rcf for 7 min at 21 °C. The pellets containing the cells were then resuspended in either McCOY's 5A medium, DMEM or MEBM, according to the cell line.

In-Cell ELISA for the detection of galectin-1 on the surface of breast cancer cells

An InCell enzyme linked immunosorbent assay (ELISA) to study the targeting ability of lactose towards the galectin-1 receptor on the surface of MDA-MB-231 and SK-BR-3 cells was performed.[46] MDA-MB-231 and SK-BR-3 cells were seeded onto a clear-bottom 96-well microplate at a concentration of 10×10^4 cells/mL (100 µL/well). The cells were incubated overnight at 37 ˚C under a 5 % CO_2 atmosphere.

The culture medium was removed and the cells were washed with PBS (100 µL) once. The nanoparticle samples, lactose-C11Pc-AuNPs and lactose-C3Pc-AuNPs (0.20 µM Pc) dissolved in FBS-free McCOY's 5A medium containing L-glutamine, were then added (50 µL/well). Additionally, a solution of staurosporine (1 mM in dimethyl sulfoxide; DMSO) dispersed in FBS-free McCOY's 5A medium containing L-glutamine (50 µL; 20 µM) was used as a positive control for cytotoxicity. Control cells not loaded with any AuNP samples were treated with FBS-free McCOY's 5A medium containing L-glutamine (50 µL). The cells were incubated with the samples and controls for 3 h at 37 °C under a 5 % CO_2 atmosphere. During the incubation period, the required buffers for the InCell ELISA were prepared following the instructions of the InCell ELISA kit.

7

Following incubation with the AuNPs, the samples were removed and the cells were washed with PBS (100 µL) three times and resuspended in McCOY's 5A medium (100 µL) containing L-glutamine and supplemented with FBS (10 %). The first part of the assay involved fixing the cells prior to addition of the primary antibody. From this point onwards, all incubation steps were performed with gentle shaking of the microplate and the plate contents were always removed using a micropipette to minimise cell loss. The culture medium was removed and formaldehyde (100 µL) was added to each well and incubated with the cells for 15 min at room temperature. The formaldehyde solution was removed and the plate was washed with 1X TBS (100 µL) twice. Permeabilization buffer (100 µL) was added to each well and incubated with the cells for 15 min at room temperature. The permeabilization buffer was removed and the cells were washed with 1X TBS (100 µL) once. Quenching solution (100 µL) was added to each well and incubated with the cells for 20 min at room temperature. The quenching solution was then removed and the cells were washed with 1X TBS (100 µL) once.

Following the fixing of the cells, blocking buffer (100 µL) was added and incubated with the cells for 30 min at room temperature. While the cells were incubated with blocking buffer, the primary anti-galectin-1 antibody was appropriately diluted to give a final concentration of 1 µg/mL. Following incubation of the cells with blocking buffer, the blocking buffer was removed with a micropipette and anti-galectin-1 antibody (50 µL; 1 µg/mL) was added to each well. The microplate was sealed with a plate sealer and the cells were incubated with the primary antibody overnight (*ca.* 17 h) at 4 °C.

The second part of the assay involved the development of an absorbance intensity signal for the levels of galectin-1 present in each sample. Following overnight incubation with the primary antibody, the blocking-washing solution was removed and the cells were washed with washing buffer (100 µL) three times. Horseradish peroxidase (HRP) conjugate (15 µL) was diluted with washing buffer (6 mL). The diluted HRP conjugate (100 µL) was added to each well and incubated with the cells for 30 min at room temperature. Following incubation, the HRP conjugate was removed and the plate was washed with washing buffer (200 µL) three times. The substrate 3,3',5,5'-tetramethylbenzidine (100 µL; TMB) was added to each well and the plate was covered with aluminium foil. The plate was then incubated for 20 min at room temperature in the dark. TMB stop solution (100 µL) was then added to stop the reaction between the TMB Substrate and the HRP conjugate. The absorbance intensity was measured at 450 nm. Background absorbance was corrected by subtracting the absorbance measurement

8

from the non-specific signal controls (*i.e.,* well not incubated with primary antibody). All samples were analysed in triplicate.

The third part of the assay involved the whole-cell staining of each well so the values of the galectin-1 receptor could be normalised to cell number. The plate contents were emptied and the plate was washed with water (200 µL) twice. Janus Green Whole-Cell Stain (100 µL) was added to each well and incubated for 5 min at room temperature. The stain was then removed and the plate was washed with water (200 µL) five times to remove all excess stain. Elution buffer (100 µL) was added to each well and incubated for 10 min at room temperature. The absorbance intensity was then measured at 615 nm. Background absorbance was corrected by subtracting the absorbance measurement from the culture medium alone. All samples were analysed in triplicate. To obtain the values of galectin-1 expression normalised to cell number in each well, the corrected absorbance values at 450 nm were divided by the corrected absorbance values at 615 nm.

Cell viability assays: CellTiter-Blue® and MTT assays

SK-BR-3, MDA-MB-231 and MCF-10A cells were seeded onto two white-bottom 96- well microplates at a concentration of 20×10^4 cells/mL (100 µL/well). The cells were incubated for *ca.* 48 h at 37 °C under a 5 % CO_2 atmosphere.

The culture medium was removed using a micropipette and the cells were washed once with PBS (100 µL). The nanoparticle samples, lactose-C11Pc-AuNPs, lactose-C3Pc-AuNPs, C11Pc-sPEG-AuNPs and C3Pc-sPEG-AuNPs, at various Pc concentrations in FBS-free McCOY's 5A medium containing L-glutamine were then added (50 µL/well). Additionally, a solution of staurosporine (1 mM in DMSO) dispersed in FBS-free McCOY's 5A medium containing L-glutamine (50 µL; 20 µM) was also used as a positive control for cytotoxicity. Control cells without any nanoparticles loaded were treated with FBS-free McCOY's 5A medium containing L-glutamine. The cells were incubated with the samples and controls for 3 h at 37 °C under a 5 % CO_2 atmosphere.

Following incubation with the functionalised nanoparticles, the samples were removed and the cells were washed with PBS (100 µL) three times. The cells were then resuspended in complete McCOY's 5A medium (100 µL) containing L-glutamine and supplemented with FBS (10 %). At this point, one of the plates was irradiated at 633 nm using a 10 mW HeNe laser fitted with a biconvex diverging lens for 6 min per well. The laser was located 50 cm above the 96-well plate,

9

giving an irradiance of 29 mW/cm^2 and a total light dose of 10.5 J/cm^2. The plate not being irradiated was kept covered in aluminium foil in the dark. The cells were further incubated for *ca.* 48 h at 37 °C under a 5 % CO_2 atmosphere prior to measuring cell viability.

CellTiter-Blue® cell viability assay: Following incubation post-PDT treatment, CellTiter-Blue® reagent (20 μL) was added to each well and incubated for 4 h at 37 °C under a 5 % CO_2 atmosphere. Fluorescence emission was then measured at 594 nm following excitation at 561 nm using a CLARIOstar® (BMG Labtech) microplate reader at room temperature. Background fluorescence was corrected by subtracting fluorescence emission from McCOY's 5A medium alone incubated with CellTiter-Blue®. Cell viability was calculated as a percentage of non-treated, non-irradiated cells. All samples were analysed in triplicate. Statistical significance between means was determined using a two-tailed Student's *t*-test and P values < 0.05 were considered significant.[47]

MTT cell viability assay: Following incubation post-PDT treatment, MTT reagent (3-(4,5,dimethylthiazol-2-yl)-2,5-diphenyltetrazolium bromide) (10 μL; 5 mg/mL in PBS) was added to each well and incubated for 4 h at 37 °C under a 5 % CO_2 atmosphere. The medium was then removed from the wells using a micropipette and the MTT formazan crystals were washed with PBS (100 μL) once and dissolved in culture-grade DMSO (200 μL). The contents of the wells were transferred to clear-bottom Nunc Nunclon™ Δ Surface 96- well microplates. The absorbance intensity was then measured at 560 nm. Background absorbance was corrected by subtracting the absorbance measurement from McCOY's 5A medium alone incubated with MTT. Cell viability and statistical significance were calculated as explained above.

Laser scanning confocal microscopy

SK-BR-3 and MDA-MB-231 cells were seeded onto 18 mm diameter glass coverslips inside 6-well multidishes at a concentration of 2×10^4 cells/mL (3 mL/well). The cells were incubated for *ca.* 48 h at 37 °C under a 5 % CO_2 atmosphere. The culture medium was removed and the cells were washed once with PBS (1 mL). Lactose-C3Pc-AuNPs (0.17 μM C3Pc) dissolved in FBS-free McCOY's 5A medium containing L-glutamine were added (1 mL/well). Control cells not loaded with nanoparticles were treated with FBS-free McCOY's 5A medium containing L-glutamine (1 mL). SK-BR-3 cells were incubated with the lactose-C3Pc-AuNPs and the control for 3 h at 37 °C under a 5 % CO_2 atmosphere. MDA-MB-231 cells were incubated with the lactose-C3Pc-AuNPs and the control for either 3 h or 24 h at 37 °C under a 5 % CO_2 atmosphere.

Following incubation with the samples, the cells were washed with PBS (1 mL) three times. They were then resuspended in complete McCOY's 5A medium (2 mL) for SK-BR-3 cells or DMEM (2 mL) for MDA-MB-231 cells. The cells were further incubated for 19 h at 37 °C under a 5 % CO_2 atmosphere. For imaging with the confocal microscope, a Carl Zeiss LSM 510 META confocal laser scanning microscope was used. The 18 mm coverslips were placed in a Ludin chamber, which was securely tightened. The cells on the coverslips were washed with imaging medium (*ca*. 1 mL) three times and finally resuspended with imaging medium (*ca.* 1 mL). The Ludin chamber was fitted on a heating stage, at 37 °C, in the confocal microscope. A 633 nm HeNe laser was used to excite the Pc on the AuNPs and the fluorescence emission was collected in the red channel with a 650 nm long pass filter. Differential interference contrast (DIC) images were collected simultaneously using a 488 nm argon-ion laser. The images were acquired with a plan-apochromat 63x/1.4 Oil DIC objective and processed using ImageJ/Fiji software.

Results and discussion

The synthesized lactose-C3Pc-AuNPs and lactose-C11Pc-AuNPs were characterized *via* TEM and UV-vis spectroscopy, as shown in **Figure 2**. Confirmation of the functionalization of the AuNPs with C3Pc or C11Pc was obtained by UV-vis spectroscopy (**Figure 2e**), which clearly shows the characteristic band of these phthalocyanines at *ca.* 698 nm.[20,40] Confirmation of the functionalization with lactose was obtained due to the facile dispersibility of the AuNPs in aqueous systems, which would otherwise be insoluble due to the hydrophobicity of the C3Pc and C11Pc. The aqueous stabilization of AuNPs with a carbohydrate, which is additionally used as a targeting agent for PDT, has not been reported previously. The lactose-C3Pc-AuNPs were found to be 3.10 ± 1.32 nm in size and the lactose-C11Pc-AuNPs were found to be 2.37 ± 1.65 nm, as analyzed by TEM (**Figure 2a-d**). The nanoparticles were evaluated for production of singlet oxygen ($^1O_2$), using the $^1O_2$ probe 9,10-anthracenediyl-bis (methylene) dimalonic acid (ABMA). Both nanoparticle systems were shown to generate $^1O_2$, as shown in **Figure 2f**, with the lactose-C3Pc-AuNPs producing more $^1O_2$ than the lactose-C11Pc-AuNPs, which is thought to be due to surface enhanced effects with the C3Pc molecule.[42]

Additionally, control AuNPs, used to evaluate the targeting ability of lactose within the lactose-C3Pc-AuNPs, were synthesized. For the control AuNPs, the lactose ligand was substituted for a polyethylene glycol ligand of a short length (sPEG), thiol-dPEG®₄-acid shown in **Figure 3a**, resembling the length of the lactose ligand. The purpose of the sPEG ligand was to facilitate the

11

solubility of the Pc-sPEG-AuNPs in aqueous solutions. Schematic representations of the synthesized gold nanoparticles functionalized with a mixed monolayer of sPEG and either C3Pc (C3Pc-sPEG-AuNPs) or C11Pc (C11Pc-sPEG-AuNPs) can be seen in **Figure 3b** and **3c**, respectively, and the UV-vis characterisation of the C3Pc-sPEG-AuNPs and C11Pc-sPEG-AuNPs, in **Figure 3d** and **3e**.
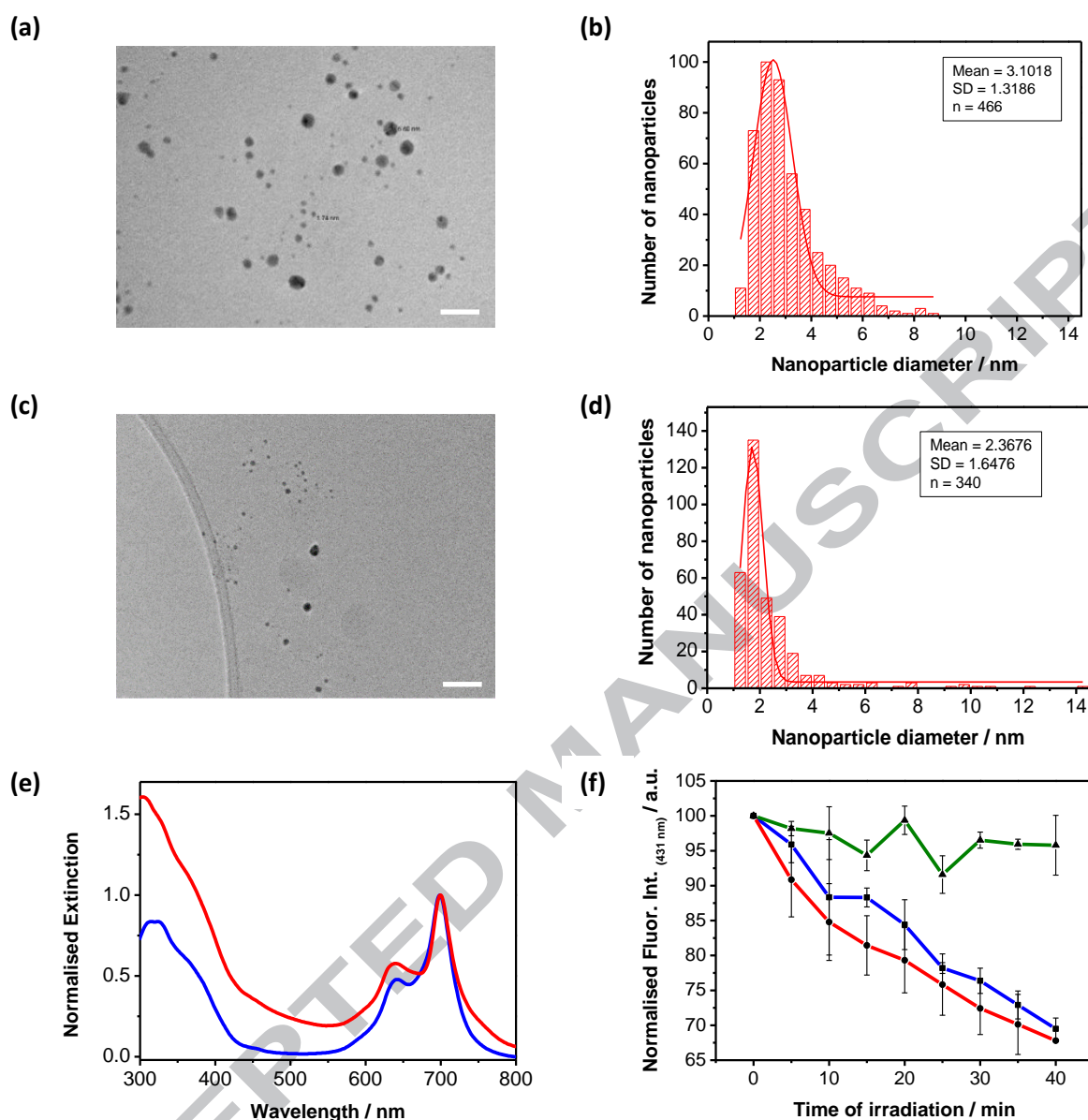
Figure 2. Characterization of the lactose-C3Pc-AuNPs and lactose-C11Pc-AuNPs. Transmission electron micrographs of a sample of **(a)** lactose-C3Pc-AuNPs and **(c)** lactose-C11Pc-AuNPs, where the scale bars represent **(a)** 20 nm and **(c)** 50 nm. Size distribution, showing the Gaussian fit, of the **(b)** lactose-C3Pc-AuNPs with an average size of 3.10 ± 1.32 nm (n = 466) and a median value of 2.72 ± 1.74 nm; and **(d)** lactose-C11Pc-AuNPs with an average size of 2.37 ± 1.65 nm (n = 340) and a median value of 1.79 ± 2.71 nm. **(e)** UV-vis extinction spectra of the synthesized lactose-C3Pc-AuNPs (red line) and lactose-C11Pc-AuNPs (blue line). **(f)** Photobleaching of ABMA in the presence of lactose-C3Pc-AuNPs (red line) and lactose-C11Pc-AuNPs (blue line) (0.734 µM) as a function of time; and no photobleaching observed for the control PEG-AuNPs (green line). Error bars represent the SD (n = 3) within a 95 % confidence interval.
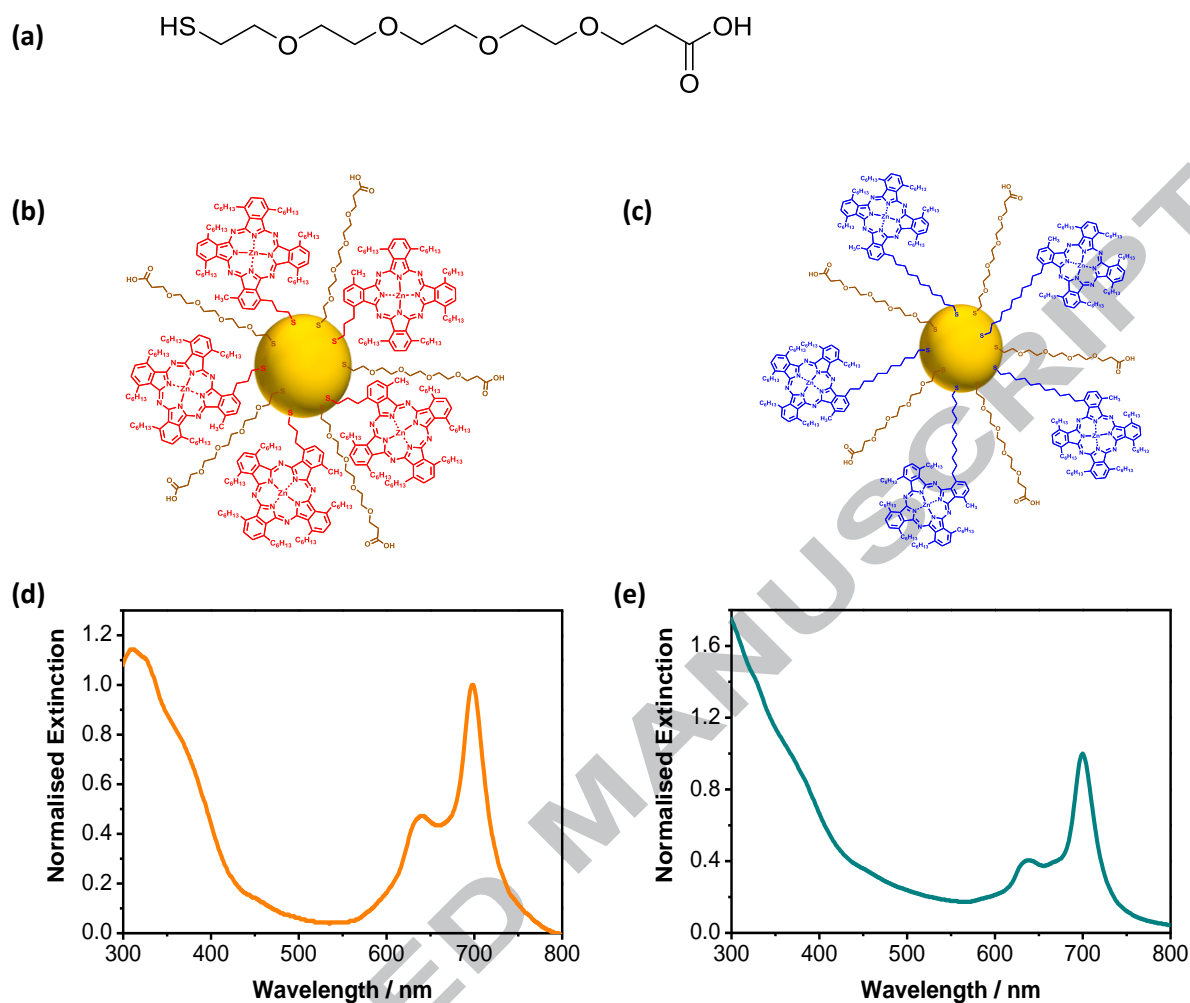
Figure 3. (a) Structure of the thiol-dPEG®$_4$-acid (sPEG)**.** Schematic representation of the **(b)** C3Pc-sPEG-AuNPs and **(c)** C11Pc-sPEG-AuNPs. UV-vis extinction spectrum of the synthesized **(d)** lactose-C3Pc-AuNPs and **(e)** lactose-C11Pc-AuNPs.

Two breast adenocarcinoma cell lines were explored, SK-BR-3 and MDA-MB-231 cells. The levels of galectin-1 on the surface of each cell line were estimated using an enzyme linked immunosorbent assay (ELISA). For this purpose, the cells were fixed and treated with anti-galectin-1 antibody.[46] The ELISA showed higher levels of galectin-1 in MDA-MB-231 cells as compared to SK-BR-3 cells (**Figure 4a**). Therefore, the MDA-MB-231 cell line was expected to be the better target for the lactose-C3Pc-AuNPs or lactose-C11Pc-AuNPs than the SK-BR-3 cell line. The potential targeting ability of lactose-C3Pc-AuNPs and lactose-C11Pc-AuNPs towards the galectin-1 receptor was then investigated in each cell line using an ELISA. To evaluate the targeting by lactose, the cells were treated with either lactose-C3Pc-AuNPs or lactose-C11Pc-

AuNPs for 3 hours and appropriately washed to remove all the non-internalized AuNPs prior to the ELISA. It was expected that the lactose would bind to the galectin-1 receptor and thus, the levels of galectin-1 on the lactose-Pc-AuNPs-treated cells would be lower than in control samples.
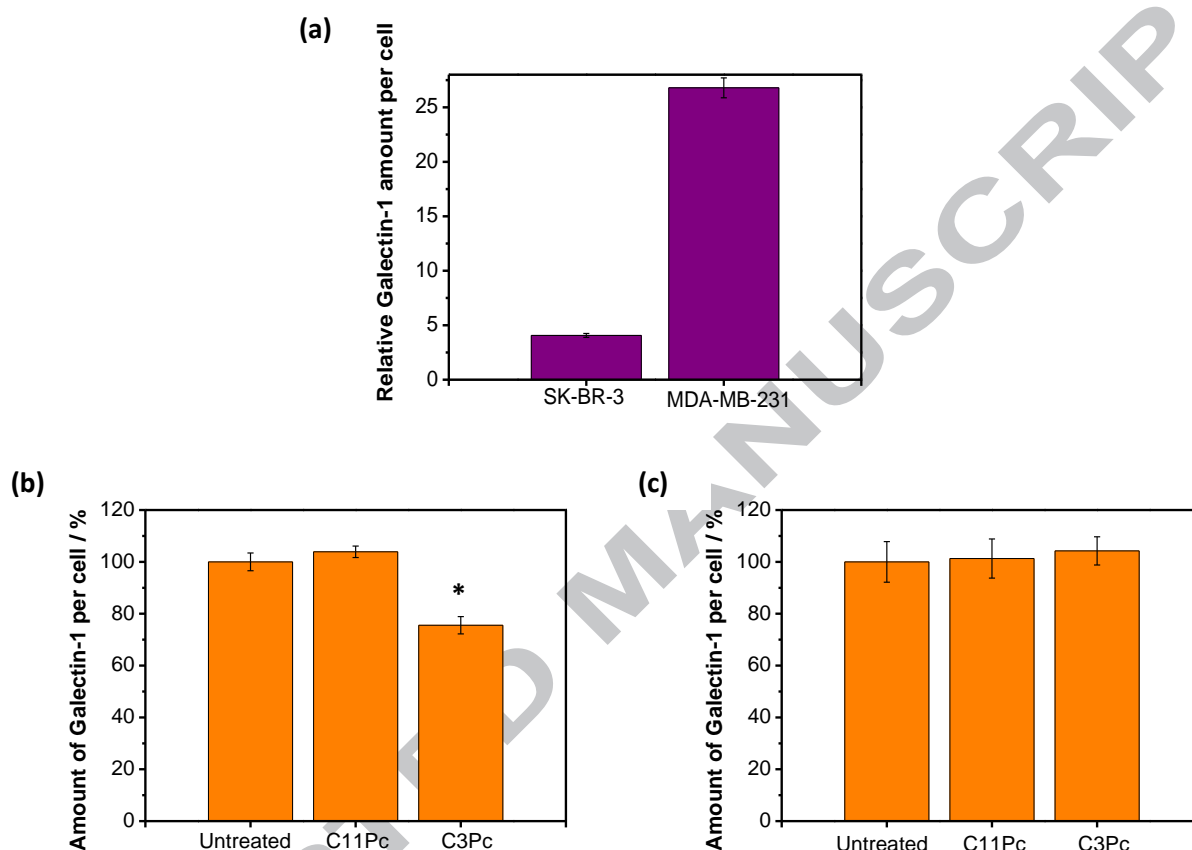

Figure 4. (a) InCell ELISA for the detection of galectin-1 on the surface of SK-BR-3 and MDA-MB-231 cells. **(b-c)** InCell ELISA for the evaluation of the targeting ability of lactose towards galectin-1 on the surface of **(b)** MDA-MB-231 cells and **(c)** SK-BR-3 cells. The samples were incubated with either lactose-C11Pc-AuNPs (C11Pc) or lactose-C3Pc-AuNPs (C3Pc) for 3 h. Figures **a-c** show the normalised values of galectin-1 per cell in each sample. Error bars represent the SD (n = 3) within a 95 % confidence interval. Statistical significance is indicated by ***** at P < 0.004, obtained using a two-tailed Student's *t*-test, where P < 0.05 is considered statistically significant.

The results, as shown in **Figure 4b-c**, indicate targeting of the galectin-1 receptor only for the MDA-MB-231 cells when they were incubated with lactose-C3Pc-AuNPs, but not the lactose-C11Pc-AuNPs. As expected from the results shown in **Figure 4a**, there is no apparent targeting of the SK-BR-3 cells for either of the nanoparticle conjugates. The fact that there is no recognition of the galectin-1 receptor on the SK-BR-3 cells does not mean that lactose will not be an

15

effective targeting ligand. There are other galactose-binding receptors on the surface of the cells. It has been reported that the glucose transporter 1 also binds galactose,[18] and thus it could be a potential targeting receptor recognised by the lactose-Pc-AuNPs. Glucose transporter 1 (GLUT1) has been reported to be overexpressed on breast cancer cells.[48–53]

With consideration that only the lactose-C3Pc-AuNPs induced selective targeting of the galectin-1 receptor, and that these nanoparticle conjugates produced more $^1O_2$ than the lactose-C11Pc-AuNPs (**Figure 2**), the lactose-C3Pc-AuNPs were studied *in vitro* using both MDA-MB-231 and SK-BR-3 cells. The cells were incubated with either lactose-C3Pc-AuNPs or the control C3Pc-sPEG-AuNPs for 24 hours, in order to maximise cell death, washed to remove all the non-internalized nanoparticles and irradiated with a 633 nm HeNe laser for 6 minutes. The cells were then subjected to CellTiter-Blue® cell viability assays to assess the PDT effect. **Figure 5a** shows the PDT effect in MDA-MB-231 cells. It can be seen that there is limited dark toxicity prior to irradiation with the laser. Additionally, post-PDT, the cell viability is reduced for samples treated with both lactose-C3Pc-AuNPs and C3Pc-sPEG-AuNPs. However, though there is an indication that the lactose-C3Pc-AuNPs could induce more cytotoxicity, with a lower cell viability post PDT, the levels of cell death are similar for both the lactose-C3Pc-AuNPs and the C3Pc-sPEG-AuNPs. This suggests that the potential targeting between lactose and galectin-1 does not lead to a great increase in cytotoxicity post-PDT. For the SK-BR-3 cells, both lactose-C3Pc-AuNPs and C3Pc-sPEG-AuNPs induce similar levels of cell death following irradiation, leading to up to 95 % cell death (**Figure 5b**). However, a clear advantage of using the lactose-C3Pc-AuNPs is highlighted by the significantly reduced dark toxicity as compared to the C3Pc-sPEG-AuNPs. Non-cancerous mammary epithelial cells, MCF-10A cells, were also subjected to PDT *via* lactose-C3Pc-AuNPs and C3Pc-sPEG-AuNPs. As it can be seen in **Figure 5c**, MCF-10A cells are not damaged by either lactose-C3Pc-AuNPs or C3Pc-sPEG-AuNPs before or after laser irradiation. The lack of cell death for non-cancerous MCF-10A cells is in contrast with the cell death obtained following PDT for cancerous MDA-MB-231 and SK-BR-3 cells. These results suggest that the presence of lactose in the lactose-C3Pc-AuNPs does not lead to an increased internalisation by non-cancerous cells, and therefore are good candidates for *in vivo* PDT of breast tumours.
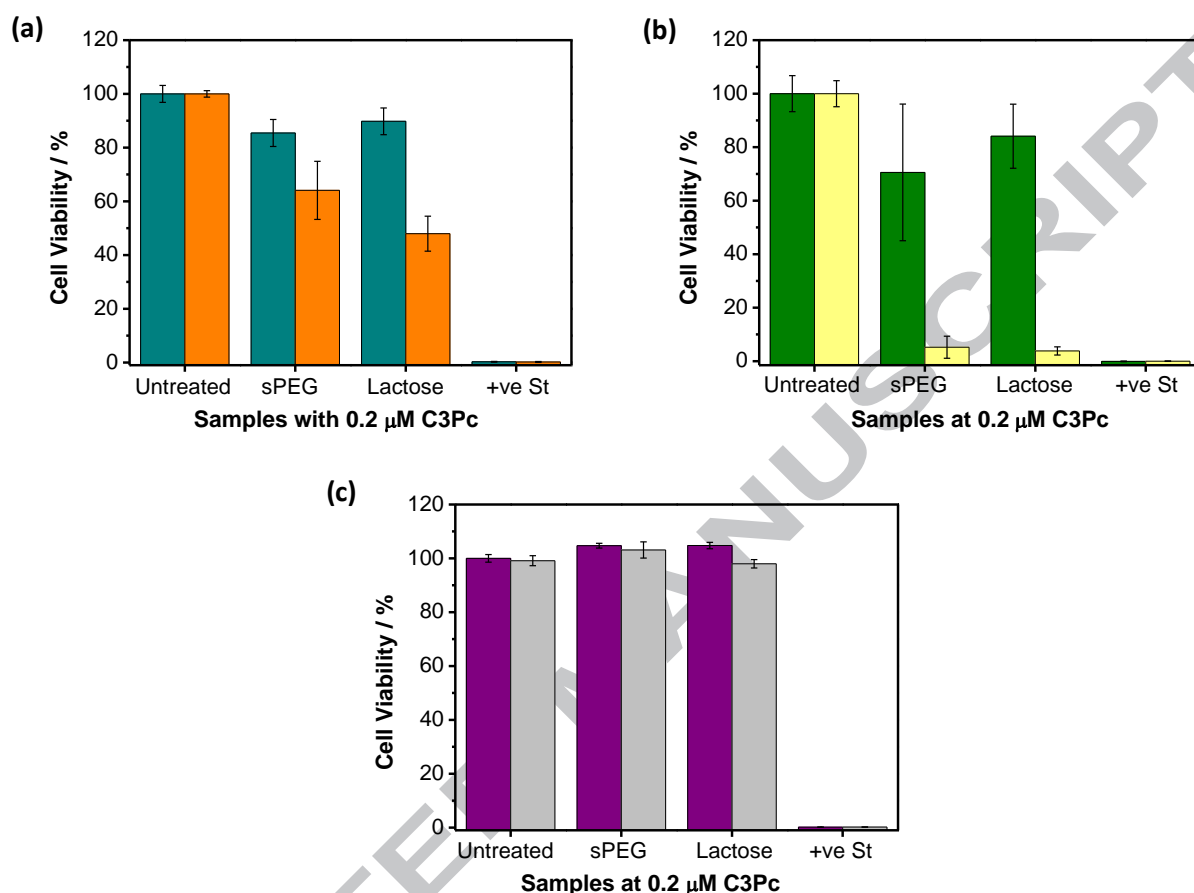
Figure 5. CellTiter-Blue® cell viability assay for **(a)** MDA-MB-231 cells, **(b)** SK-BR-3 cells and **(c)** MCF-10A cells incubated with C3Pc-sPEG-AuNPs (sPEG) or lactose-C3Pc-AuNPs (lactose) for 24 h. Untreated refers to cells only treated with growth medium. Cells were either irradiated with a 633 nm HeNe laser (**a**) orange, **b)** light yellow, **c)** grey) or non-irradiated (**a**) dark cyan, **b)** green, **c)** purple). Staurosporine (+ve St) was used as a positive control for cytotoxicity. Error bars represent the SD (n = 3) within a 95 % confidence interval. No statistically significant difference between C3Pc-sPEG-AuNPs and lactose-C3Pc-AuNPs, as indicated by the P values (**a)** P < 0.09; **b)** P < 0.1) obtained using a two-tailed Student's *t*-test, where P < 0.05 is considered statistically significant.

Given that SK-BR-3 cells incubated with either lactose-C3Pc-AuNPs or C3Pc-sPEG-AuNPs at 0.2 µM C3Pc for 24 h induce high levels of cytotoxicity, it is difficult to confirm that there is targeting *via* lactose. Therefore, a study of lower concentrations of C3Pc and different incubation periods (*i.e.,* 3 h) would show whether there is any selective targeting due to the presence of the lactose on the nanoparticles. **Figure 6** shows that lactose-C3Pc-AuNPs target the SK-BR-3 cells at lower

17

concentrations (0.05 μM C3Pc), as the cell death is statistically significantly different between lactose-C3Pc-AuNPs (97 %; **Figure 6a**) and C3Pc-sPEG-AuNPs (75 %; **Figure 6b**).
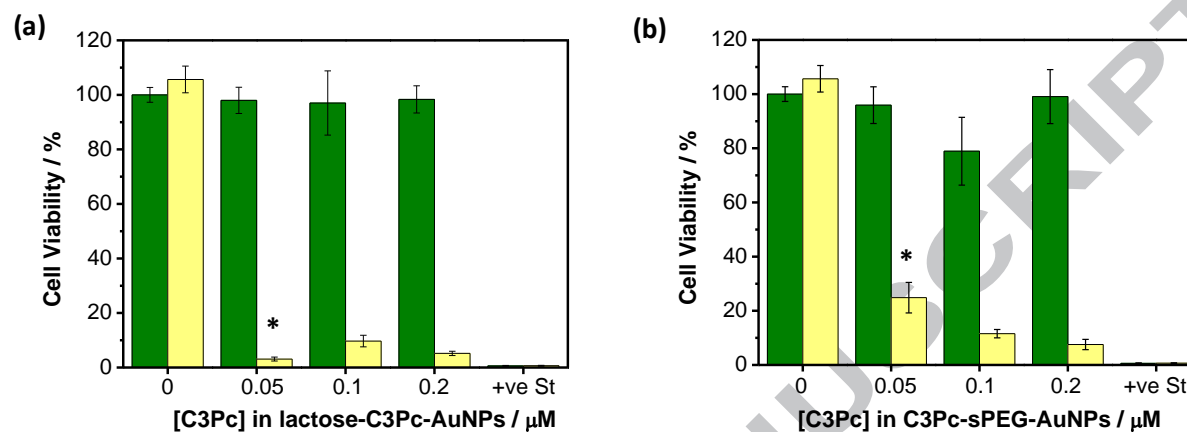

Figure 6. CellTiter-Blue® cell viability assay for SK-BR-3 cells incubated with **(a)** lactose-C3Pc-AuNPs or **(b)** C3Pc-sPEG-AuNPs (sPEG) for 3 h. Cells were either irradiated with a 633 nm HeNe laser (light yellow) or non-irradiated (green). Staurosporine (+ve St) was used as a positive control for cytotoxicity. Error bars represent the SD ($n = 3$) within a 95 % confidence interval. Statistically significant difference between C3Pc-sPEG-AuNPs and lactose-C3Pc-AuNPs (0.05 μM C3Pc) is indicated by * at $P < 0.003$, obtained using a two-tailed Student's *t*-test, where $P < 0.05$ is considered statistically significant. At higher concentrations, the difference is not statistically significant ($P < 0.2$).

Even though the targeting ability of lactose towards the galectin-1 receptor in MDA-MB-231 cells only leads to a limited increase in cell death (**Figure 5a**), it can be clearly seen that the lactose-C3Pc-AuNPs are good candidates for PDT of breast cancer cells. The internalisation of the lactose-C3Pc-AuNPs is efficient by both MDA-MB-231 cells and SK-BR-3 cells, as shown by confocal microscopy (**Figure 7**). Additionally, it has been shown that the lactose-C3Pc-AuNPs induce effective cell death, especially when treating the SK-BR-3 cell line.
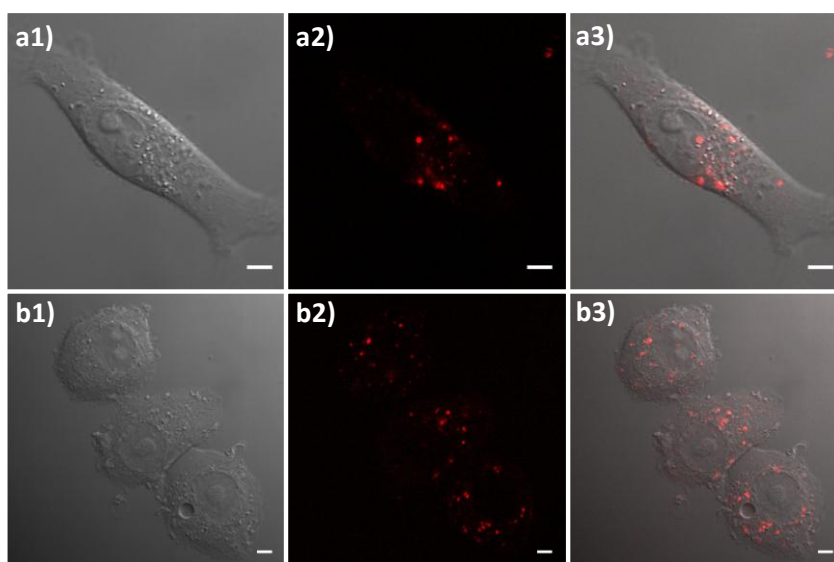
Figure 7. Confocal fluorescence microscopy images of **(a)** MDA-MB-231 and **(b)** SK-BR-3 cells incubated with lactose-C3Pc-AuNPs for either **(a)** 24 h or **(b)** 3 h. The samples were imaged 24 h following incubation. Images taken from: **1)** DIC, **2)** fluorescence from C3Pc collected in the red channel (λ_{ex} = 633 nm; above 650 nm), **3)** composite images of DIC and fluorescence from C3Pc collected in the red channel. Scale bars represent 10 μm.

Given the positive results seen with the lactose-C3Pc-AuNPs, it was decided to study the synthesized lactose-C11Pc-AuNPs (**Figure 1c**) *in vitro* to assess any potential targeting *via* lactose towards receptors other than galectin-1 on the surface of the MDA-MB-231 or SK-BR-3 cells. Initial cell viability studies with various concentrations of C11Pc within the AuNPs were performed, to evaluate the optimal concentration to be used for PDT. For this purpose, only SK-BR-3 cells were incubated with the lactose-C11Pc-AuNPs for 24 h and irradiated with a 633 nm HeNe laser for 6 minutes. **Figure 8** clearly shows that the optimal concentration for these type of nanoparticles is 0.25 μM, as it showed minimal dark toxicity while some cell kill could be seen post PDT. Higher concentrations of the C11Pc (0.5 and 0.7 μM) led to cytotoxicity prior to cell irradiation so these concentrations were not used for PDT treatment.
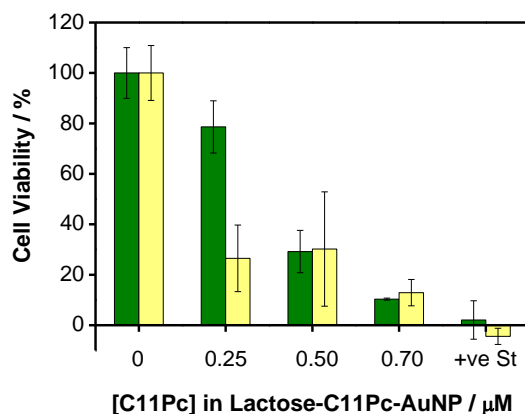
19

Figure 8. MTT cell viability assay for SK-BR-3 cells incubated with various concentrations of lactose-C11Pc-AuNPs for 24 h. Cells were either irradiated with a 633 nm HeNe laser (light yellow) or non-irradiated (green). Staurosporine (+ve St) was used as a positive control for cytotoxicity.

Once the optimal concentration (0.25 µM, C11Pc) for PDT was determined, the cells were incubated with either lactose-C11Pc-AuNPs or C11Pc-sPEG-AuNPs for 24 hours, washed to remove all the non-internalized nanoparticles and irradiated with a 633 nm HeNe laser for 6 minutes. The cells were then subjected to CellTiter-Blue® cell viability assays to assess the PDT effect. **Figure 9a** shows the effect in MDA-MB-231 cells. It can be seen that there is no cell death either before or after irradiation (*i.e.,* post-PDT). For the SK-BR-3 cells, **Figure 9b**, both the lactose-C11Pc-AuNPs and C11Pc-sPEG-AuNPs induce cell death following irradiation with negligible dark toxicity. Furthermore, the lactose-C11Pc-AuNPs induce more cytotoxicity (90 %) than the C11Pc-sPEG-AuNPs (61 %) post-PDT. This is an indication that the lactose-C11Pc-AuNPs are selectively targeting the SK-BR-3 cells, even though it appears not related to the galectin-1 receptor (**Figure 4**). Other galactoside-binding receptors overexpressed on breast cancer cells, such as GLUT1, could be responsible for this selective targeting.
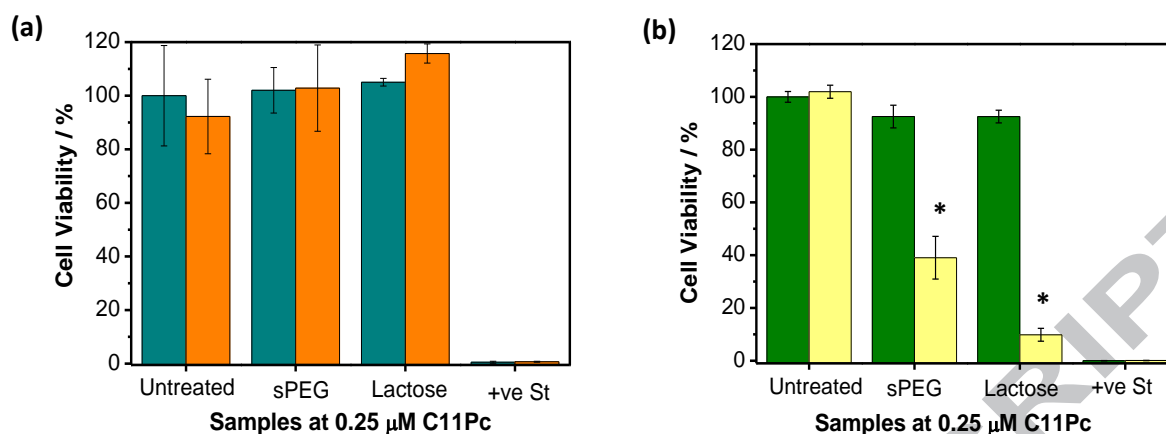
Figure 9. CellTiter-Blue® cell viability assay for **(a)** MDA-MB-231 cells and **(b)** SK-BR-3 cells incubated with C11Pc-sPEG-AuNPs (sPEG) or lactose-C11Pc-AuNPs (lactose) for 24 h. Untreated refers to cells only treated with growth medium. Cells were either irradiated with a 633 nm HeNe laser (**a)** orange, **b)** yellow) or non-irradiated (**a)** dark cyan, **b)** green). Staurosporine (+ve St) was used as a positive control for cytotoxicity. Error bars represent the SD (n = 3) within a 95 % confidence interval. A statistically significant difference between C11Pc-sPEG-AuNPs and lactose-C11Pc-AuNPs is indicated by ***** at P < 0.006, obtained using a two-tailed Student's *t*-test, where P < 0.05 is considered statistically significant.

A study of concentrations of C11Pc with the lactose-C11Pc-AuNPs and C11Pc-sPEG-AuNPs (< 0.2 μM) did not achieve any cell death post PDT. These results are in contrast with the results seen for lower concentrations of the lactose-C3Pc-AuNPs and C3Pc-sPEG-AuNPs (see **Figure 6**). Overall, the results reported here show that the lactose-C3Pc-AuNPs perform better than the lactose-C11Pc-AuNPs with both types of breast cancer cells studied.

Conclusions

In summary, we have shown that phthalocyanine functionalized gold nanoparticles can be stabilized and dispersed in aqueous solutions using a lactose derivative. These lactose-phthalocyanine functionalized gold nanoparticles are biocompatible and good candidates for *in vitro* and, ultimately, *in vivo* PDT. The ability of the synthesized lactose functionalized gold nanoparticles to target the galectin-1 receptor overexpressed on some breast cancer cells was studied. For this purpose, two zinc phthalocyanine photosensitizers, C3Pc and C11Pc, were used to evaluate their PDT efficacy *in vitro*. It was shown that the galectin-1 receptor overexpressed on the surface of MDA-MB-231 cells can be targeted only *via* lactose-C3Pc-AuNPs, whereas

lactose-C11Pc-AuNPs do not appear to show any targeting ability. However, the use of either nanoparticles did not show any targeting *via* galectin-1 with SK-BR-3 cells. This result is consistent with the finding that SK-BR-3 cells do not overexpress galectin-1.

In vitro PDT studies using the lactose-C3Pc-AuNPs were performed with both cell lines, MDA-MB-231 and SK-BR-3 cells. Although targeting of the lactose-C3Pc-AuNPs towards galectin-1 was observed for the MDA-MB-231 cells, it did not correlate with an increase in cell death post PDT. Indeed, the cell death achieved was comparable to the control non-targeted C3Pc-sPEG-AuNPs. By contrast, SK-BR-3 cells were killed more efficiently by lactose-C3Pc-AuNPs (97 % cell death at 0.05 μM C3Pc) than the control C3Pc-sPEG-AuNPs (75 % cell death at 0.05 μM C3Pc), indicating that lactose was selectively targeting the SK-BR-3 cells. Even though the targeting ability of the lactose-C3Pc-AuNPs in SK-BR-3 appears to be unrelated to the galectin-1 receptor, the presence of other targeting receptors on the cell surface should be studied to understand how this selective interaction is enhancing photodynamic therapy of breast cancer cells. *In vitro* PDT studies using the lactose-C11Pc-AuNPs showed comparable results to those observed with the lactose-C3Pc-AuNPs. The synthesized lactose-C11Pc-AuNPs were shown to induce no targeting towards the galectin-1 receptor on the MDA-MB-231 cells, thus leading to no internalization and no cell death post-PDT. However, the use of the lactose-C11Pc-AuNPs indicated targeting towards the SK-BR-3 cells, leading to significant levels of cytotoxicity (90 % at 0.2 μM C11Pc) as compared to the control C11Pc-sPEG-AuNPs (61 % at 0.2 μM C11Pc). These results suggest that the C3Pc photosensitizer should be used in preference to the C11Pc photosensitizer, given that it induces higher levels of cytotoxicity for both cell lines, at a lower photosensitizer concentration.

This study shows that lactose can be successfully used to target breast cancer cells. The use of a carbohydrate as a targeting agent has several advantages over other biomolecules such as antibodies. Cancer cells can become resistant to antibodies due to genetic mutations, leading to innate or acquired resistance towards the treatment, as seen for the use of Herceptin to treat HER2 positive breast cancers.[54,55] Additionally, the present study has shown enhanced cell kill compared to previous work where other carbohydrates have been used for selective cancer targeting.[13,15] More importantly, we have successfully increased levels of cell death with lower irradiation periods and radiation doses (29 mW/cm^2; 10.5 J/cm^2 for 6 minutes) to those reported previously (50 mW/cm^2; 90 J/cm^2 for 30 minutes).[13]

22

In conclusion, the results reported show that the use of lactose to stabilize the hydrophobic phthalocyanine photosensitizer on the gold nanoparticles in aqueous solutions has clear advantages for targeted photodynamic therapy and suggests that other carbohydrates should be investigated for optimal targeting of ligands on cancer cells.

Acknowledgements

Keywords

Photodynamic therapy · targeting · gold nanoparticles · carbohydrates · galectin-1 · zinc phthalocyanines
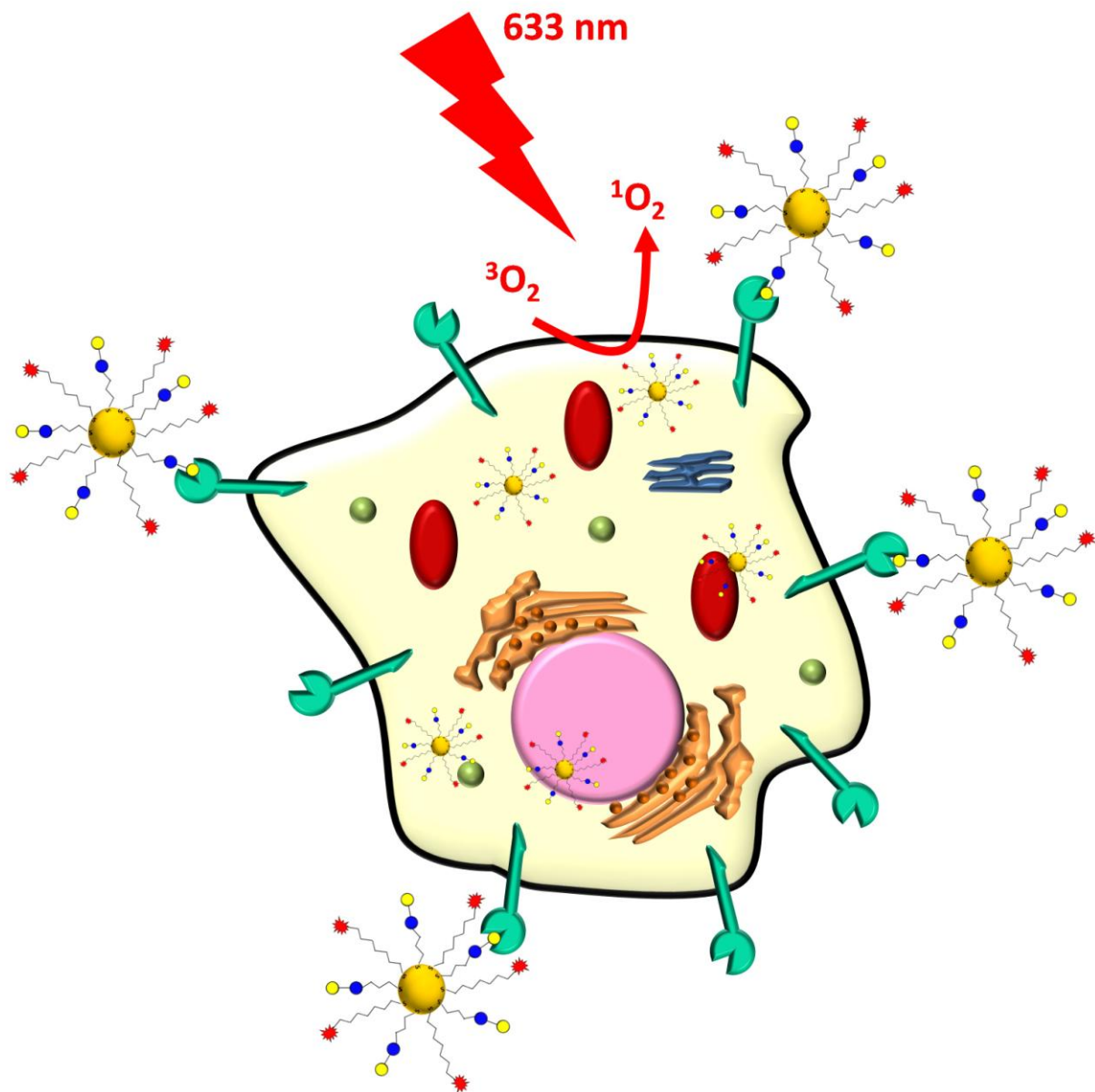
References

[1]   P. Nangia-Makker, J. Conklin, V. Hogan, A. Raz, Carbohydrate-binding proteins in cancer, and their ligands as therapeutic agents, Trends Mol. Med. 8 (2002) 187–192.

[2]   I. Häuselmann, L. Borsig, Altered tumor-cell glycosylation promotes metastasis, Front. Oncol. 4 (2014) 1–15.

[3]   H. Ghazarian, B. Idoni, S. B. Oppenheimer, A glycobiology review: carbohydrates, lectins and implications in cancer therapeutics, Acta Histochem. 113 (2011) 236–247.

[4]   A. Varki, Biological role of glycans, Glycobiology 27 (2017) 3–49.

[5]   F. M. Tuccillo, A. De Laurentiis, C. Palmieri, G. Fiume, P. Bonelli, A. Borrelli, P. Tassone, I. Scala, F. M. Buonaguro, I. Quinto, G. Scala, Aberrant glycosylation as biomarker for cancer: focus on CD43, Biomed Res. Int. 2014 (2014) 742831–742844.

[6]   S. S. Pinho, C. A. Reis, Glycosylation in cancer: mechanisms and clinical implications, Nat. Rev. Cancer 15 (2015) 540–555.

[7]   D. H. Dube, C. R. Bertozzi, Glycans in cancer and inflammation – potential for therapeutics and diagnostics, Nat. Rev. Drug Discov. 4 (2005) 477–488.

[8]   D. L. Meany, D. W. Chan, Aberrant glycosylation associated with enzymes as cancer biomarkers, Clin. Proteomics 8 (2011) 7–21.

[9]   T. Minko, Drug targeting to the colon with lectins and neoglycoconjugates, Adv. Drug Deliv. Rev. 56 (2004) 491–509.

[10]   K. Cho, X. Wang, S. Nie, Z. Chen, D. M. Shin, Therapeutic nanoparticles for drug delivery in cancer, Clin. Cancer Res. 14 (2008) 1310–1316.

[11]   R. Sinha, G. J. Kim, S. Nie, D. M. Shin, Nanotechnology in cancer therapeutics:

bioconjugated nanoparticles for drug delivery, Am. Assoc. Cancer Res. 5 (2006) 1909–1917.

[12]   D. Brevet, M. Gary-Bobo, L. Raehm, S. Richeter, O. Hocine, K. Amro, B. Loock, P. Couleaud, C. Frochot, A. Morère, P. Maillard, M. Garcia, J. O. Durand, Mannose-targeted mesoporous silica nanoparticles for photodynamic therapy, Chem. Commun. (2009) 1475–1477.

[13]   M. Gary-Bobo, Y. Mir, C. Rouxel, D. Brevet, O. Hocine, M. Maynadier, A. Gallud, A. Da Silva, O. Mongin, M. Blanchard-Desce, S. Richeter, B. Loock, P. Maillard, A. Morère, M. Garcia, L. Raehm, J. O. Durand, Multifunctionalized mesoporous silica nanoparticles for the in vitro treatment of retinoblastoma: drug delivery, one and two photon photodynamic therapy, Int. J. Pharm. 432 (2012) 99–104.

[14]   M. Gary-Bobo, Y. Mir, C. Rouxel, D. Brevet, I. Basile, M. Maynadier, O. Vaillant, O. Mongin, M. Blanchard-Desce, A. Morère, J. O. Durand, L. Raehm, Mannose-functionalized mesoporous silica nanoparticles for efficient two-photon photodynamic therapy of solid tumors, Angew. Chem. Int. Ed. 50 (2011) 11425–11429.

[15]   M. Gary-Bobo, O. Hocine, D. Brevet, M. Maynadier, L. Raehm, S. Richeter, V. Charasson, B. Loock, A. Morère, P. Maillard, M. Garcia, J. O. Durand, Cancer therapy improvement with mesoporous silica nanoparticles combining targeting, drug delivery and PDT, Int. J. Pharm. 423 (2012) 509–515.

[16]   M. Perrier, M. Gary-Bobo, L. Lartigue, D. Brevet, A. Morère, M. Garcia, P. Maillard, L. Raehm, Y. Guari, J. Larionova, J. O. Durand, O. Mongin, M. Blanchard-Desce, Mannose-functionalized porous silica-coated magnetic nanoparticles for two-photon imaging or PDT of cancer cells, J. Nanoparticle Res. 15 (2013) 1602–619.

[17]   D. C. Kennedy, G. Orts-Gil, C.-H. Lai, L. Müller, A. Haase, A. Luch, P. H. Seeberger, Carbohydrate functionalization of silver nanoparticles modulates cytotoxicity and cellular uptake, J. Nanobiotechnology 12 (2014) 59–66.

[18]   P. M. R. Pereira, S. Silva, J. A. S. Cavaleiro, C. A. F. Ribeiro, J. P. C. Tomé, R. Fernandes, Galactodendritic phthalocyanine targets carbohydrate-binding proteins enhancing photodynamic therapy, PLoS One 9 (2014) 22–30.

[19]   J. Peng, K. Wang, W. Tan, X. He, C. He, P. Wu, F. Liu, Identification of live liver cancer cells in a mixed cell system using galactose-conjugated fluorescent nanoparticles, Talanta 71 (2007) 833–840.

[20]   G. Obaid, I. Chambrier, M. J. Cook, D. A. Russell, Targeting the oncofetal Thomsen-Friedenreich disaccharide using jacalin-PEG phthalocyanine gold nanoparticles for photodynamic cancer therapy, Angew. Chem. Int. Ed. 51 (2012) 6158–6162.

[21]   M. V. Dwek, H. A. Ross, A. J. Streets, S. A. Brooks, E. Adam, A. Titcomb, J. V. Woodside, U. Schumacher, A. J. Leathem, Helix pomatia agglutinin lectin-binding oligosaccharides of aggressive breast cancer, Int. J. Cancer 95 (2001) 79–85.

[22]   X. Gao, T. Wang, B. Wu, J. Chen, J. Chen, Y. Yue, N. Dai, H. Chen, X. Jiang, Quantum dots for tracking cellular transport lectin-functionalized nanoparticles, Biochem. Biophys. Res. Commun. 377 (2008) 35–40.

[23]   C. Wang, P. C. Ho, L. Y. Lim, Wheat germ agglutinin-conjugated PLGA nanoparticles for enhanced intracellular delivery of paclitaxel to colon cancer cells, Int. J. Pharm. 400 (2010) 201–210.

[24]   J. Wang, T. Duan, L. Sun, D. Liu, Z. Wang, Functional gold nanoparticles for studying the interaction of lectin with glycosyl complex on living cellular surfaces, Anal. Biochem. 392 (2009) 77–82.

[25]   J. A. Ochoa-Alvarez, H. Krishnan, Y. Shen, N. K. Acharya, M. Han, D. E. McNulty, H.

Hasegawa, T. Hyodo, T. Senga, J. G. Geng, M. Kosciuk, S. S. Shin, J. S. Goydos, D. Temiakov, R. G. Nagele, G. S. Goldberg, Plant lectin can target receptors containing sialic acid, exemplified by podoplanin, to inhibit transformed cell growth and migration, PLoS One 7 (2012) e41845–e41496.

[26]   S. M. Hussain, L. K. Braydich-Stolle, A. M. Schrand, R. C. Murdock, K. O. Yu, D. M. Mattie, J. J. Schlager, Toxicity evaluation for safe use of nanomaterials: recent achievements and technical challenges, Adv. Mater. 21 (2009) 1549–1559.

[27]   S. H. Barondes, D. N. W. Cooper, M. A. Gitt, H. Leffler, Galectins. Structure and function of a large family of animal lectins, J. Biol. Chem. 269 (1994) 20807–20810.

[28]   A. Danguy, I. Camby, R. Kiss, Galectins and cancer, Biochim. Biophys. Acta - Gen. Subj. 1572 (2002) 285–293.

[29]   E. Gorelik, U. Galili, A. Raz, On the role of cell surface carbohydrates and their binding proteins (lectins) in tumor metastasis, Cancer Metastasis Rev. 20 (2001) 245–277.

[30]   G. A. Rabinovich, Galectins: an evolutionarily conserved family of animal lectins with multifunctional properties; a trip from the gene to clinical therapy, Cell Death Differ. 6 (1999) 711–721.

[31]   L. Astorgues-Xerri, M. E. Riveiro, A. Tijeras-Raballand, M. Serova, C. Neuzillet, S. Albert, E. Raymond, S. Faivre, Unraveling galectin-1 as a novel therapeutic target for cancer, Cancer Treat. Rev. 40 (2014) 307–319.

[32]   K. Ito, K. Stannard, E. Gabutero, A. M. Clark, S. Y. Neo, S. Onturk, H. Blanchard, S. J. Ralph, Galectin-1 as a potent target for cancer therapy: role in the tumor microenvironment, Cancer Metastasis Rev. 31 (2012) 763–778.

[33]   V. Balan, P. Nangia-Makker, A. Raz, Galectins as cancer biomarkers, Cancers 2 (2010) 592–610.

[34]   T. Dalotto-Moreno, D. O. Croci, J. P. Cerliani, V. C. Martinez-Allo, S. Dergan-Dylon, S. P. Méndez-Huergo, J. C. Stupirski, D. Mazal, E. Osinaga, M. A. Toscano, V. Sundblad, G. A. Rabinovich, M. Salatino, Targeting galectin-1 overcomes breast cancer-associated immunosuppression and prevents metastatic disease, Cancer Res. 73 (2013) 1107–1117.

[35]   R. Bhat, B. Belardi, H. Mori, P. Kuo, A. Tam, W. C. Hines, Q.-T. Le, C. R. Bertozzi, M. J. Bissell, Nuclear repartitioning of galectin-1 by an extracellular glycan switch regulates mammary morphogenesis, Proc. Natl. Acad. Sci. U. S. A. 113 (2016) e4820–e4827.

[36]   N. L. Perillo, M. E. Marcus, L. G. Baum, Galectins: versatile modulators of cell adhesion, cell proliferation, and cell death, J. Mol. Med. 76 (1998) 402–412.

[37]   D. Demydenko, I. Berest, Expression of galectin-1 in malignant tumors, Exp. Oncol. 31 (2009) 74–79.

[38]   M. L. Louka, H. Said, S. El Sayed, M. El-Shinawi, Galectin 1 overexpression in breast cancer tissues: Relation to serum matrix metalloproteinase 2 and 9 activity, Gene Reports 7 (2017) 184–188.

[39]   G. A. Rabinovich, Galectin-1 as a potential cancer target, Br. J. Cancer 92 (2005) 1188–92.

[40]   T. Stuchinskaya, M. Moreno, M. J. Cook, D. R. Edwards, D. A. Russell, Targeted photodynamic therapy of breast cancer cells using antibody-phthalocyanine-gold nanoparticle conjugates, Photochem. Photobiol. Sci. 10 (2011) 822–831.

[41]   G. Obaid, I. Chambrier, M. J. Cook, D. A. Russell, Cancer targeting with biomolecules: A comparative study of photodynamic therapy efficacy using antibody or lectin conjugated phthalocyanine-PEG gold nanoparticles, Photochem. Photobiol. Sci. 14 (2015) 737–747.

[42]   P. García Calavia, M. J. Marín, I. Chambrier, M. J. Cook, D. A. Russell, Towards

optimisation of surface enhanced photodynamic therapy of breast cancer cells using gold nanoparticle-photosensitiser conjugates, Photochem. Photobiol. Sci. (2017).

[43] A. J. Reynolds, A. H. Haines, D. A. Russell, Gold glyconanoparticles for mimics and measurement of metal ion-mediated carbohydrate-carbohydrate interactions, Langmuir 22 (2006) 1156–1163.

[44] I. Chambrier, M. J. Cook, D. A. Russell, Synthesis and characterisation of functionalised phthalocyanine compounds for fabrication of self-assembled monolayers, Synthesis 10 (1995) 1283–1286.

[45] D. J. Revell, I. Chambrier, M. J. Cook, D. A. Russell, Formation and spectroscopic characterisation of self-assembled phthalocyanine monolayers, J. Mater. Chem. 10 (2000) 31–37.

[46] Thermo Fisher Scientific. InCell ELISA Colorimetric Detection Kit – Catalog number 62200 https://www.thermofisherscientific.com/oder/catalog/product/62200 [Accessed Jun 23rd, 2017].

[47] L. Rodriguez, P. Vallercosa, S. Battah, G. Di Venosa, G. Calvo, L. Mamone, D. Sáenz, M. C. Gonzalez, A. Batlle, A. J. MacRobert, A. Casas, Aminolevulinic acid dendrimers in photodynamic treatment of cancer and atheromatous disease, Photochem. Photobiol. Sci. 14 (2015) 1617–1627.

[48] A. Krzeslak, K. Wojcik-Krowiranda, E. Forma, P. Jozwiak, H. Romanowicz, A. Bienkiewicz, M. Brys, Expression of GLUT1 and GLUT3 glucose transporters in endometrial and breast cancers, Pathol. Oncol. Res. 18 (2012) 721–728.

[49] R. S. Brown, R. L. Wahl, Overexpression of glut1 glucose transporter in human breast cancer, Cancer 72 (1993) 2979–2985.

[50] C. D. Young, A. S. Lewis, M. C. Rudolph, M. D. Ruehle, M. R. Jackman, U. J. Yun, O. Ilkun, R. Pereira, E. D. Abel, S. M. Anderson, Modulation of glucose transporter 1 (GLUT1) expression levels alters mouse mammary tumor cell growth in vitro and in vivo, PLoS One 6 (2011) e23205–e23216.

[51] M. Grover-McKay, S. A. Walsh, E. A. Seftor, P. A. Thomas, M. J. Hendrix, Role for glucose transporter 1 protein in human breast cancer, Pathol. Oncol. Res. 4 (1998) 115–120.

[52] L. Venturelli, S. Nappini, M. Bulfoni, G. Gianfranceschi, S. Dal Zilio, G. Coceano, F. Del Ben, M. Turetta, G. Scoles, L. Vaccari, D. Cesselli, D. Cojoc, Glucose is a key driver for GLUT1-mediated nanoparticles internalization in breast cancer cells, Sci. Rep. 6 (2016) 21629–21642.

[53] Y. R. Hussein, S. Bandyopadhyay, A. Semaan, Q. Ahmed, B. Albashiti, T. Jazaerly, Z. Nahleh, R. Ali-Fehmi, Glut-1 expression correlates with basal-like breast cancer, Transl. Oncol. 4 (2011) 321–327.

[54] Z. Sun, Y. Shi, Y. Shen, L. Cao, W. Zhang, X. Guan, Analysis of different HER-2 mutations in breast cancer progression and drug resistance, J. Cell. Mol. Med. 19 (2015) 2691–2701.

[55] P. R. Pohlmann, I. A. Mayer, R. Mernaugh, Resistance to trastuzumab in breast cancer, Clin. Cancer Res. 15 (2009) 7479–7491.